

Review: mechanism of oscillation

Necessary condition: negative feedback to carry a reaction network back to the ‘starting point’ of its oscillation.

Additional condition 1: the negative feedback signal must be sufficiently delayed in time to destabilize the steady state.

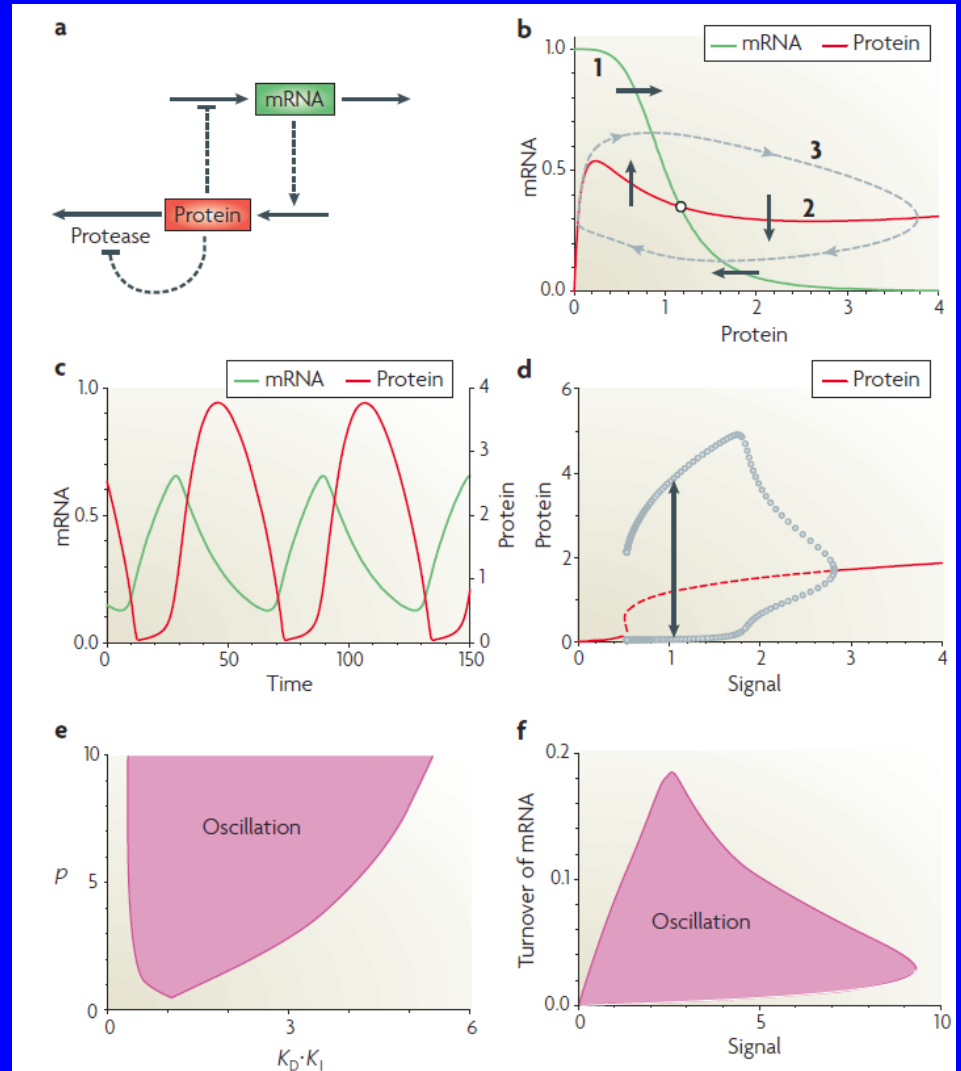
Additional condition 2: the kinetic rate laws of the reaction mechanism must be sufficiently ‘nonlinear’ to destabilize the steady state.

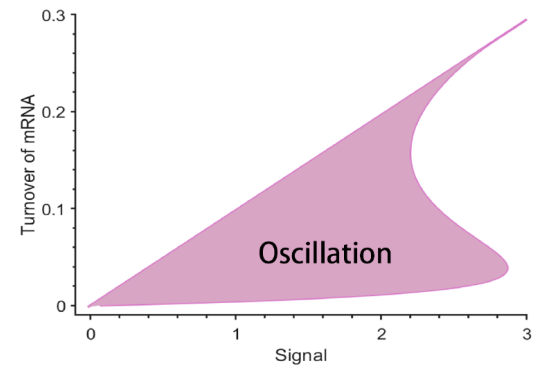
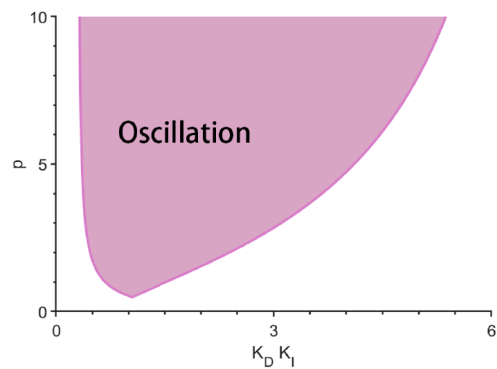
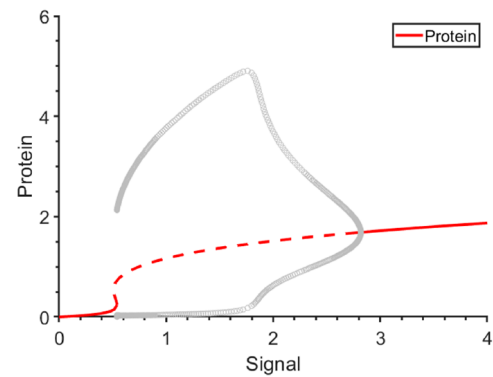
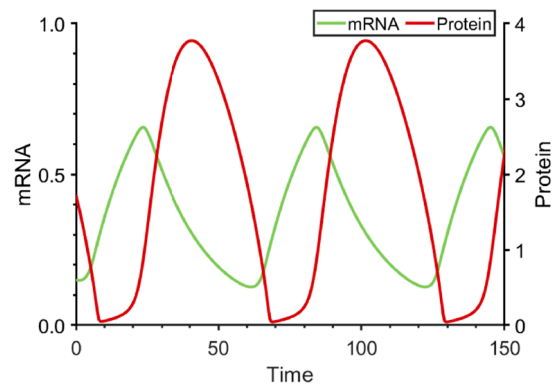
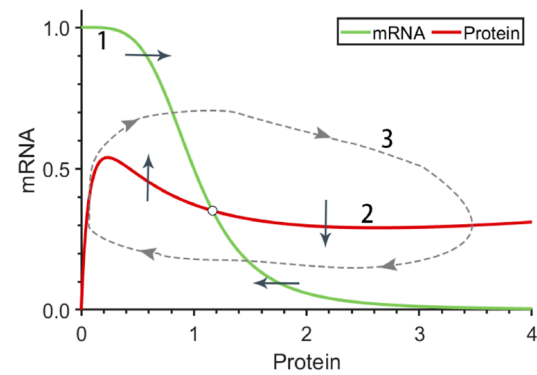
Additional condition 3: production and consumption reactions must occur on appropriate timescales.

Comment on homework

Figure 4

Novak, B. and J. J. Tyson
(2008). Nat Rev Mol Cell Biol 9(12): 981-991.





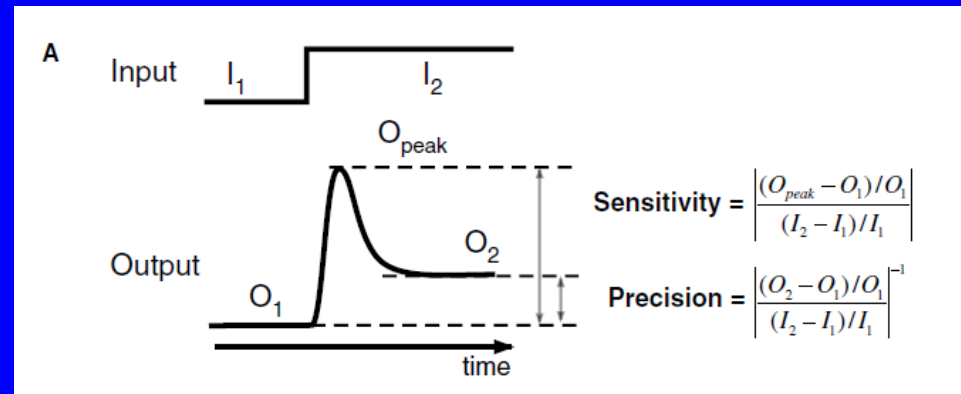
3.2 Perfect adaptation

Definition: (Biochemical adaptation)

Adaptation refers to the system's ability to respond to a change in input stimulus then return to its prestimulated output level, even when the change in input persists.

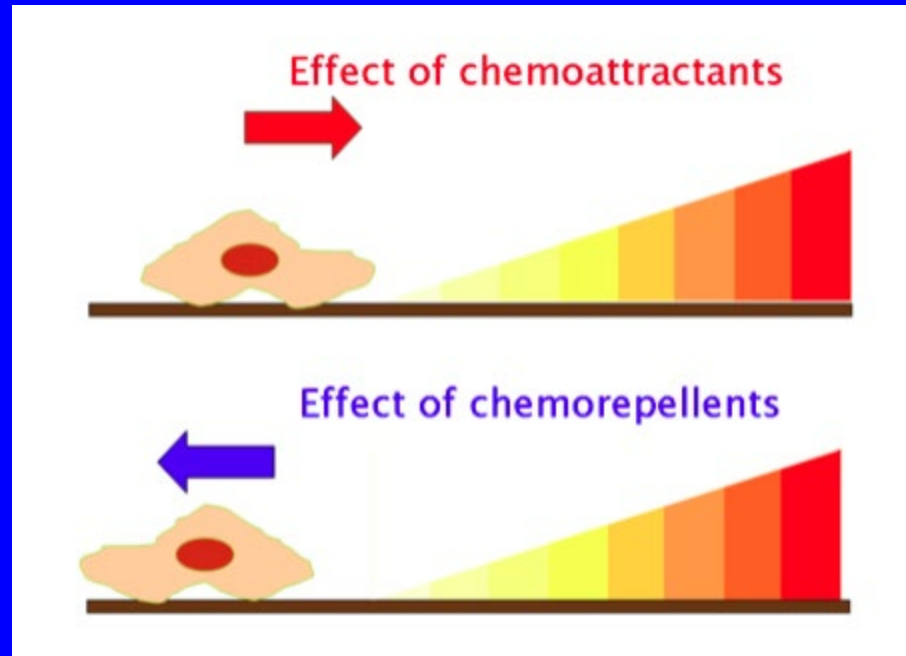
Adaptation is commonly used in sensory and other signaling networks to expand the input range that a circuit is able to sense.

Ma W, Trusina A, El-Samad H, Lim WA, Tang C. .2009; **138**(4): 760-73.



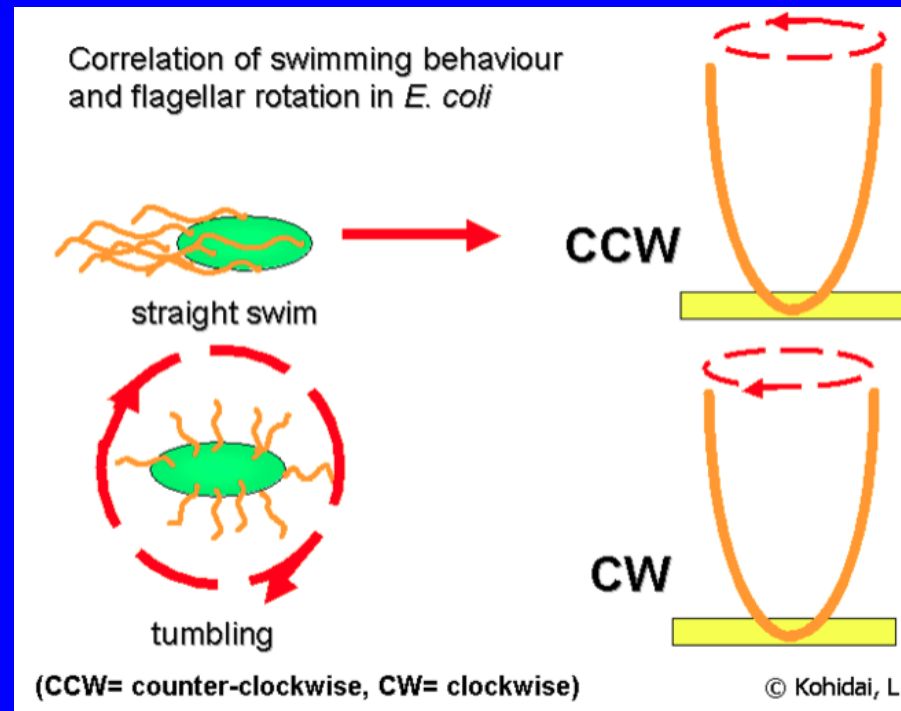
Adaptation in bacteria chemotaxis

Chemotaxis (from *chemo-* + *taxis*) is the movement of an organism in response to a chemical stimulus. Somatic cells, bacteria, and other single-cell or multicellular organisms direct their movements according to certain chemicals in their environment.

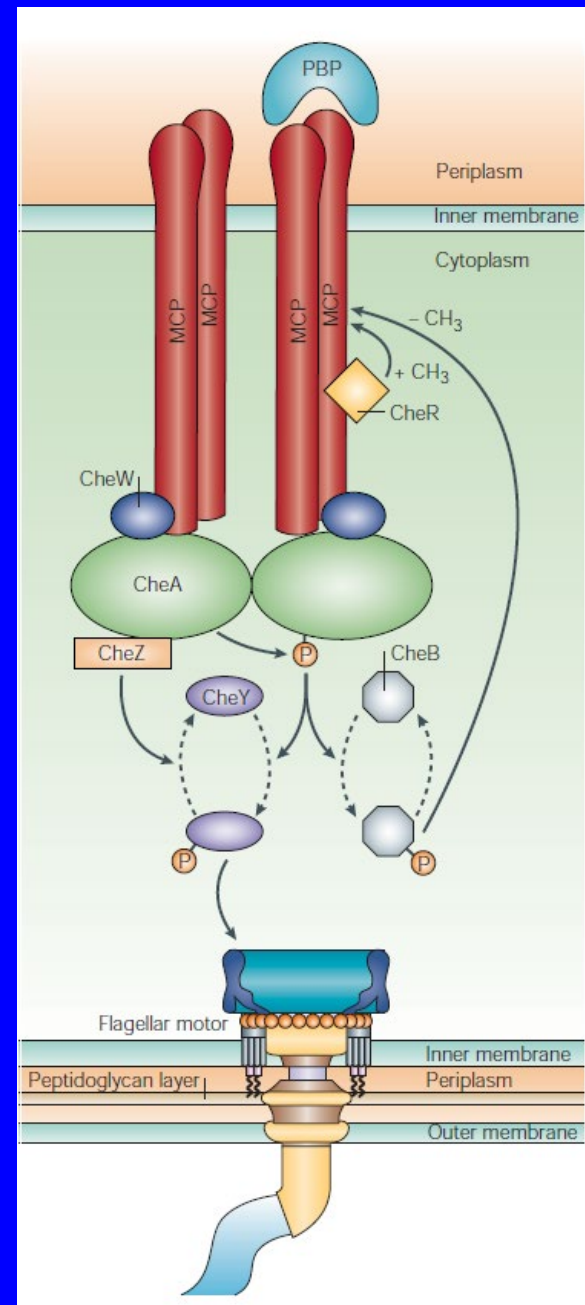


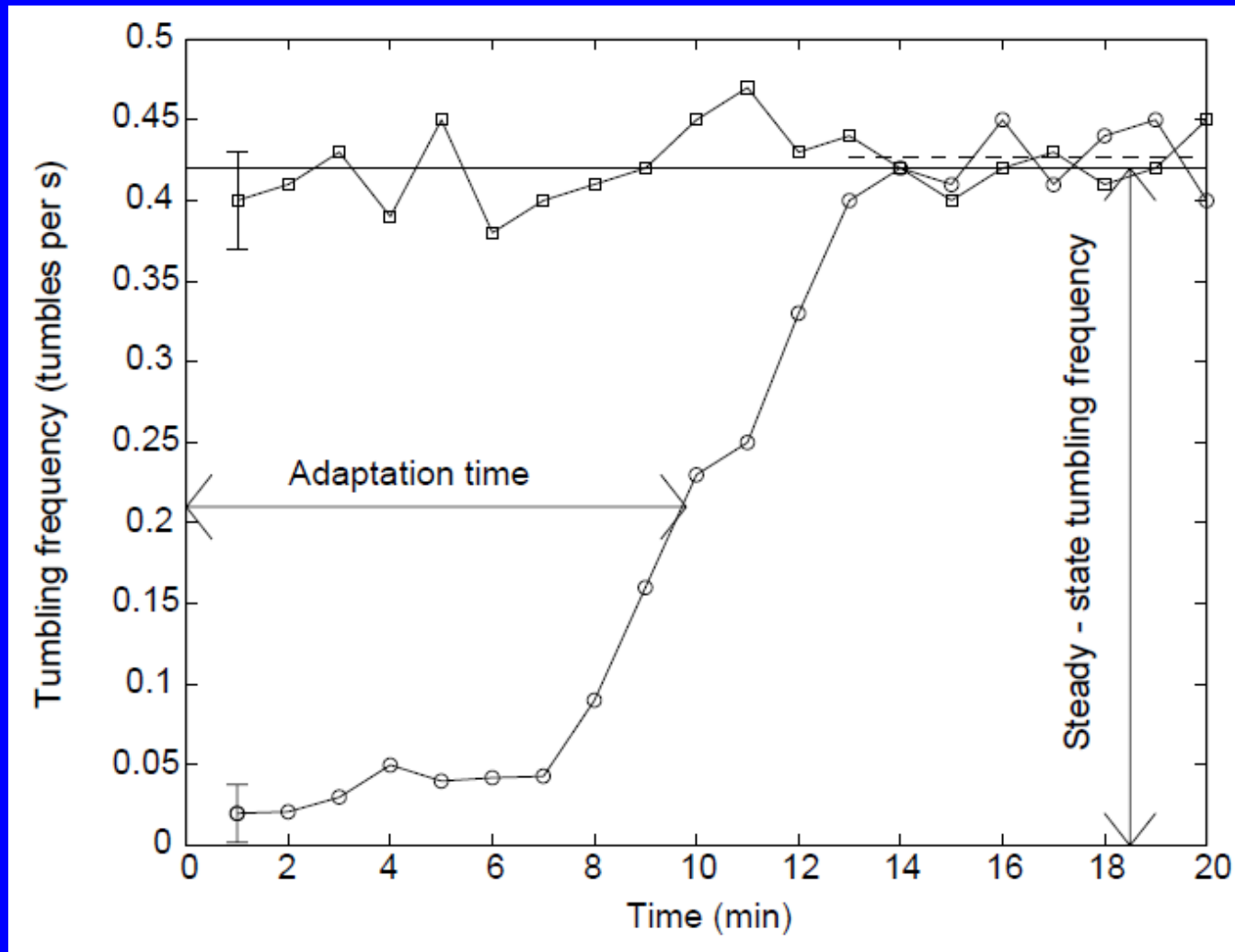
Chemotaxis system of *E. coli*

Bacterial motion resembles a random walk, with periods of smooth swimming interrupted by brief tumbles that change the swimming direction.



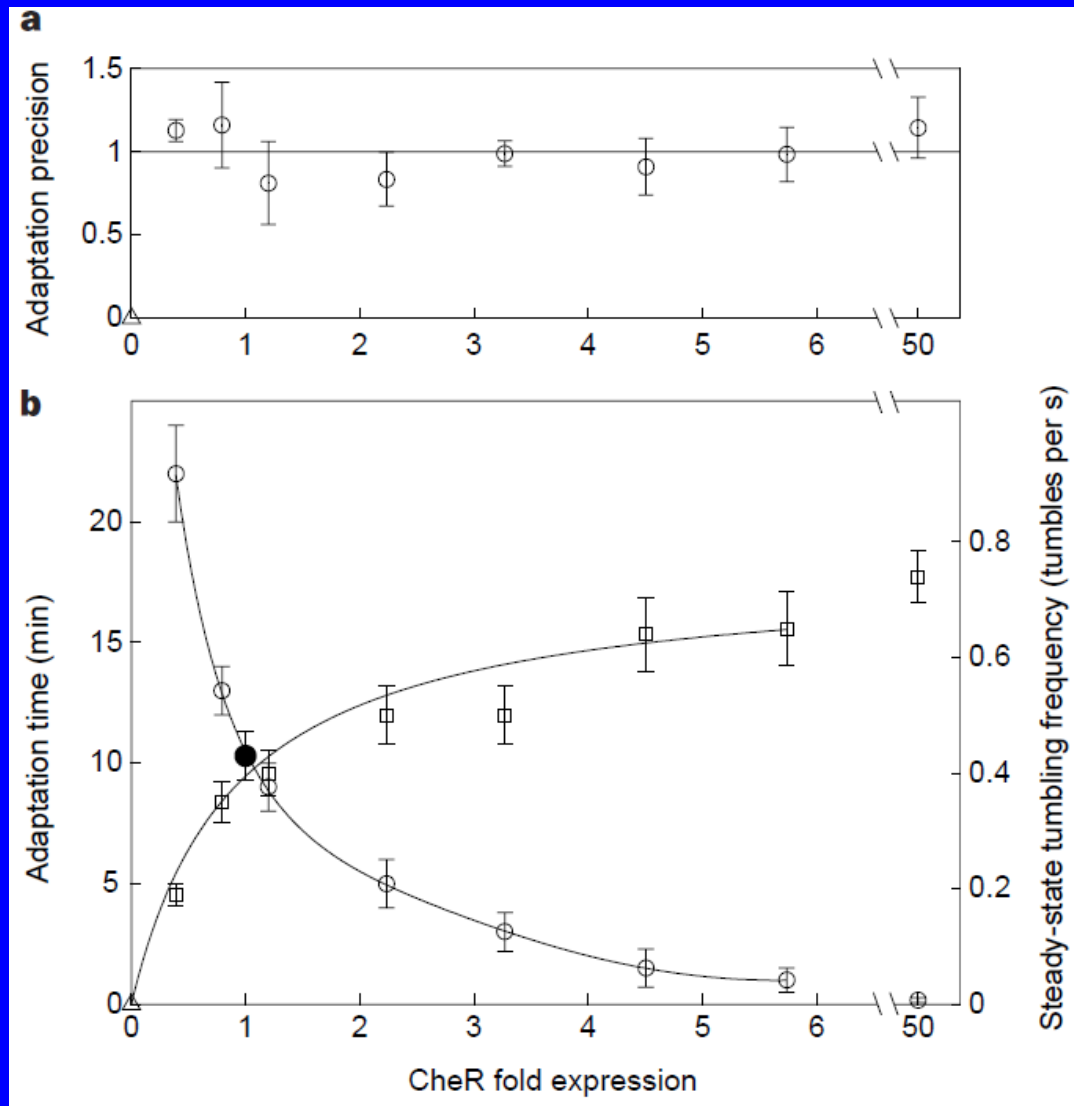
CheA phosphorylates itself and then transfers phosphoryl (P) groups to CheY (Y), a diffusible messenger protein. The phosphorylated form of CheY interacts with the Flagellar motors to induce tumbles. The rate of CheY dephosphorylation is greatly enhanced by CheZ (Z). Adaptation is provided by changes in the level of methylation of the chemoreceptors: methylation increases the rate of CheY phosphorylation. A pair of enzymes, CheR (R) and CheB (B), add and remove methyl (m) groups.





Tumbling frequency as a function of time for wild-type cells.

Alon, U., M. G. Surette, N. Barkai and S. Leibler (1999). [Nature 397\(6715\): 168-171.](#)



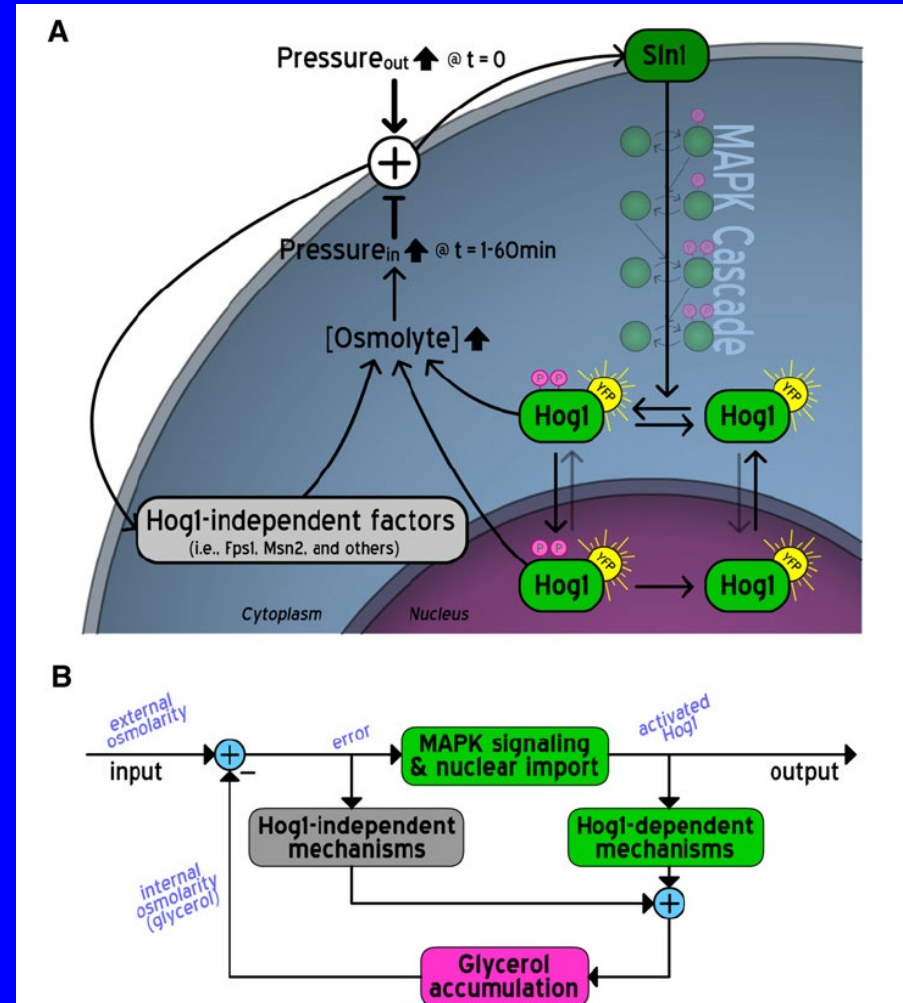
Chemotaxis behavior of cells with varying intracellular concentration of the protein CheR.

Summary

We focus on how response and adaptation to attractant signals vary with systematic changes in the intracellular concentration of the components of the chemotaxis network. We find that some properties, such as steady-state behavior and adaptation time, show strong variations in response to varying protein concentrations. In contrast, the precision of adaptation is robust and does not vary with the protein concentrations.

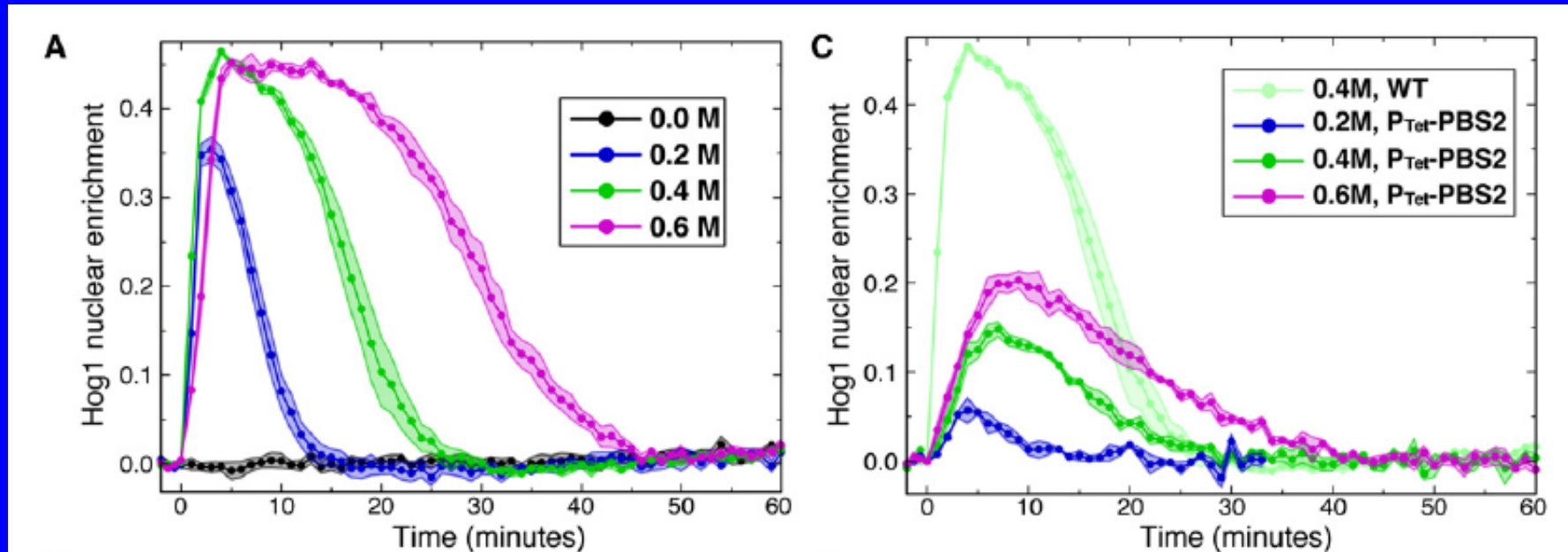
Hog1 Translocates to the Nucleus in Response to Hyperosmotic Shock

An upward spike in external osmotic pressure at $t = 0$ is sensed by Sln1, which propagates a signal via a MAPK cascade that culminates in the dual phosphorylation and nuclear import of Hog1. In the nucleus, Hog1 activates gene expression; active Hog1 also plays various roles in the cytoplasm to facilitate osmo-adaptation.



Muzzey, D., C. A. Gómez-Urbe, et al. (2009). Cell 138(1): 160-171.

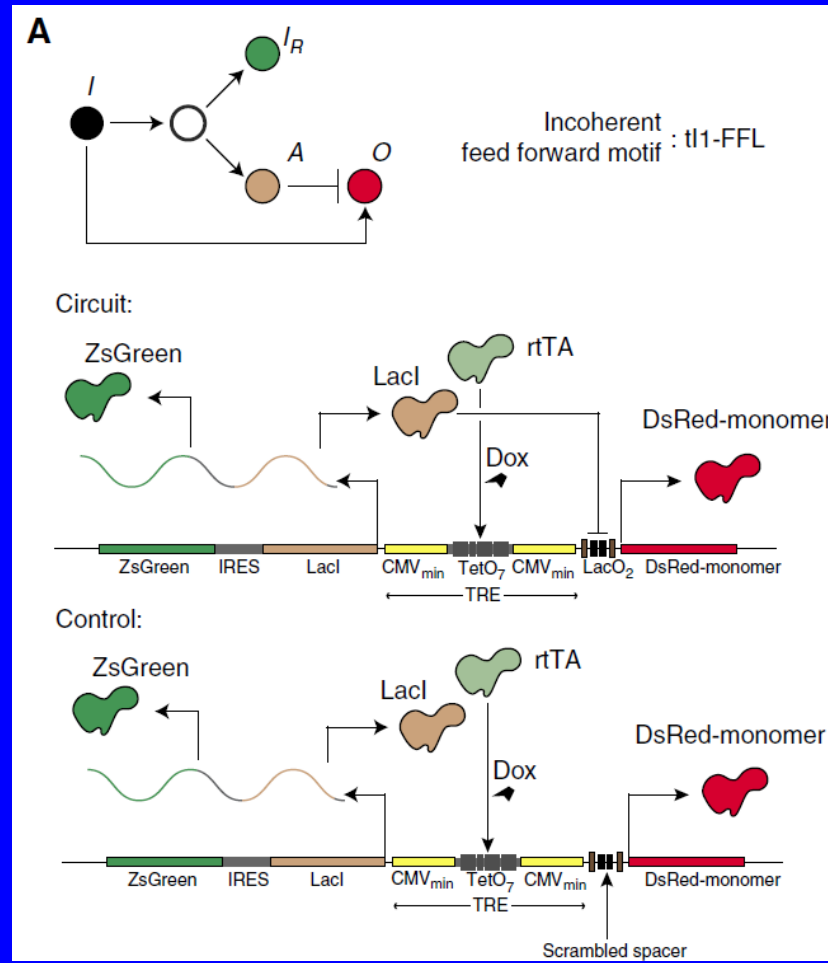
A Systems-Level Analysis of Perfect Adaptation in Yeast Osmoregulation



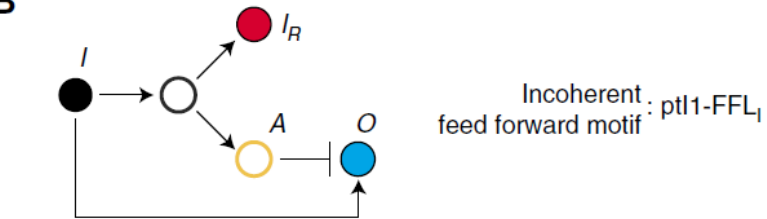
Hog1 Nuclear Enrichment Exhibits Robust Perfect Adaptation

Muzzey, D., C. A. Gómez-Urbe, et al. (2009). Cell **138**(1): 160-171.

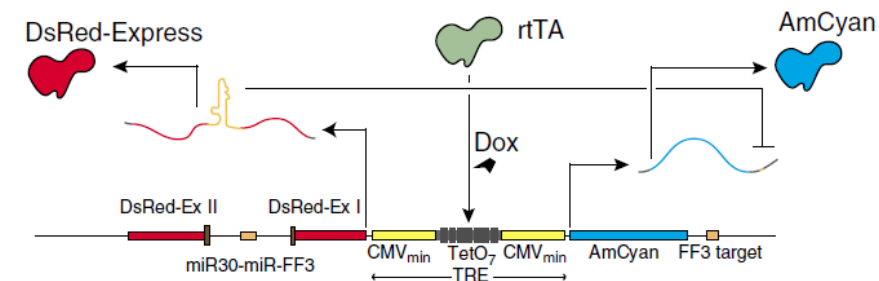
Adaptation in Synthetic incoherent feedforward circuits



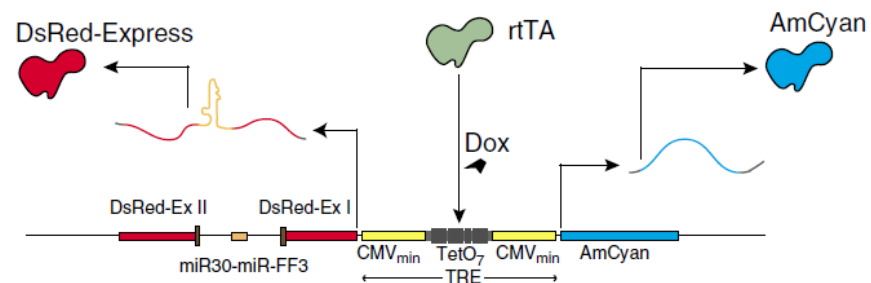
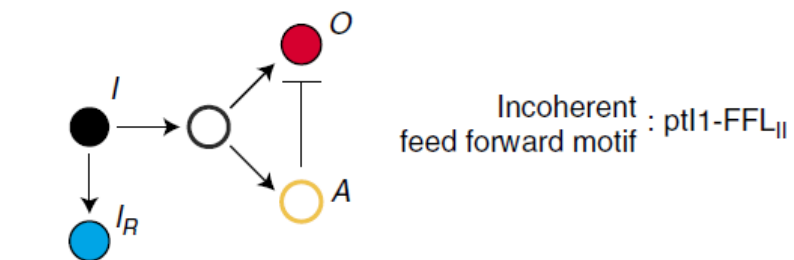
Bleris, L., Z. Xie, et al. (2011). Mol Syst Biol 7.

B

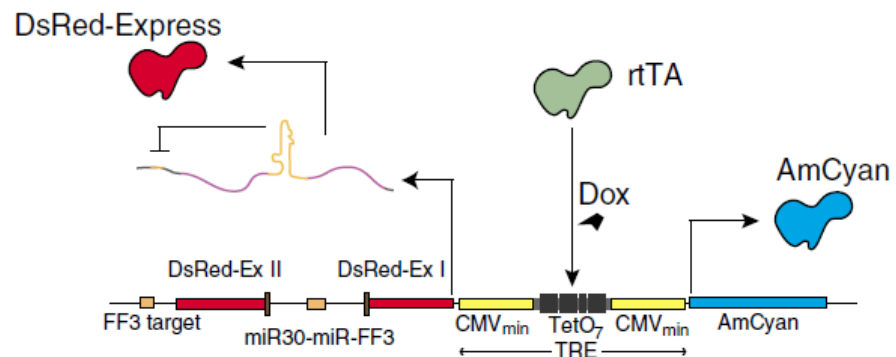
Circuit:

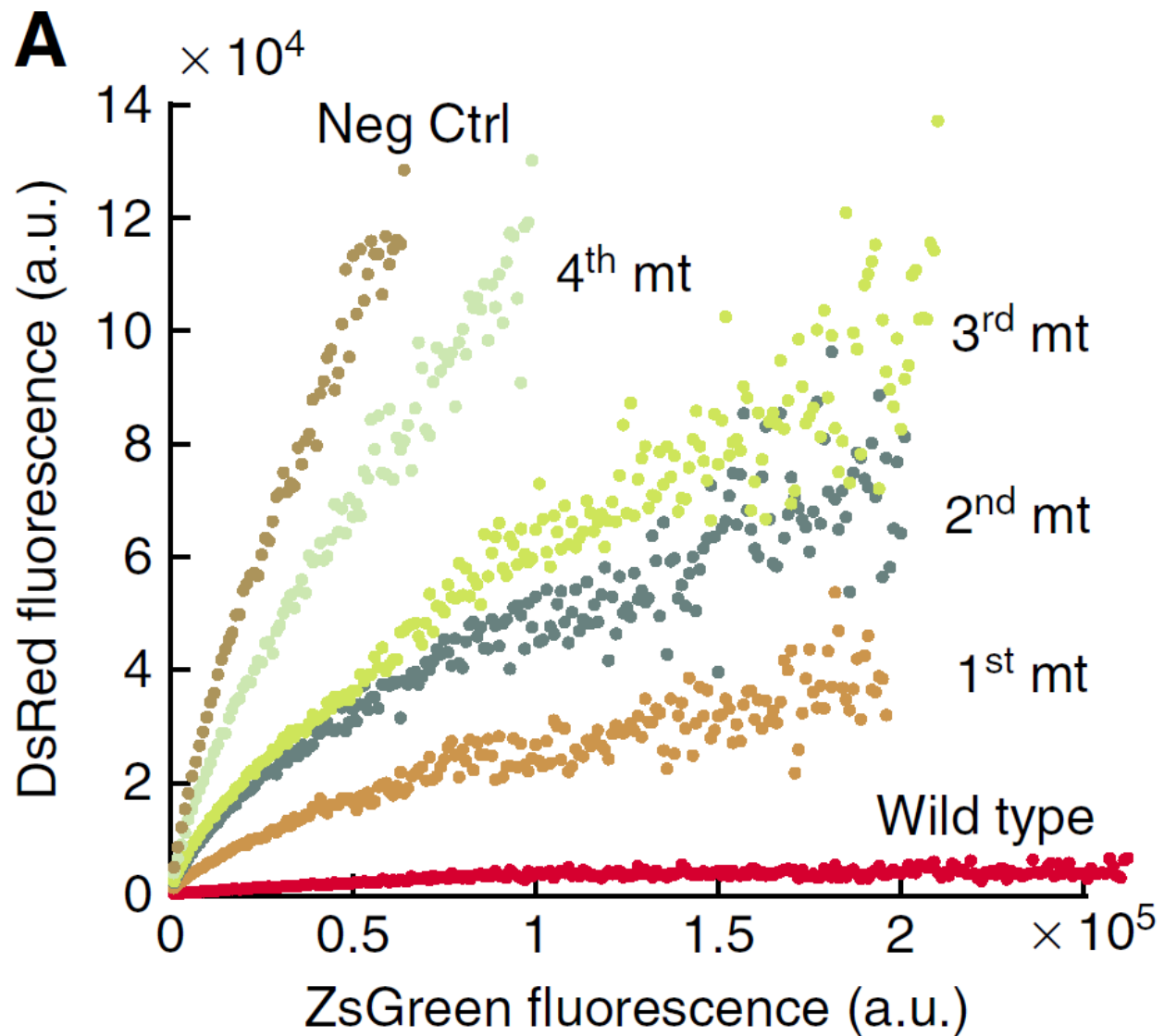


Control:

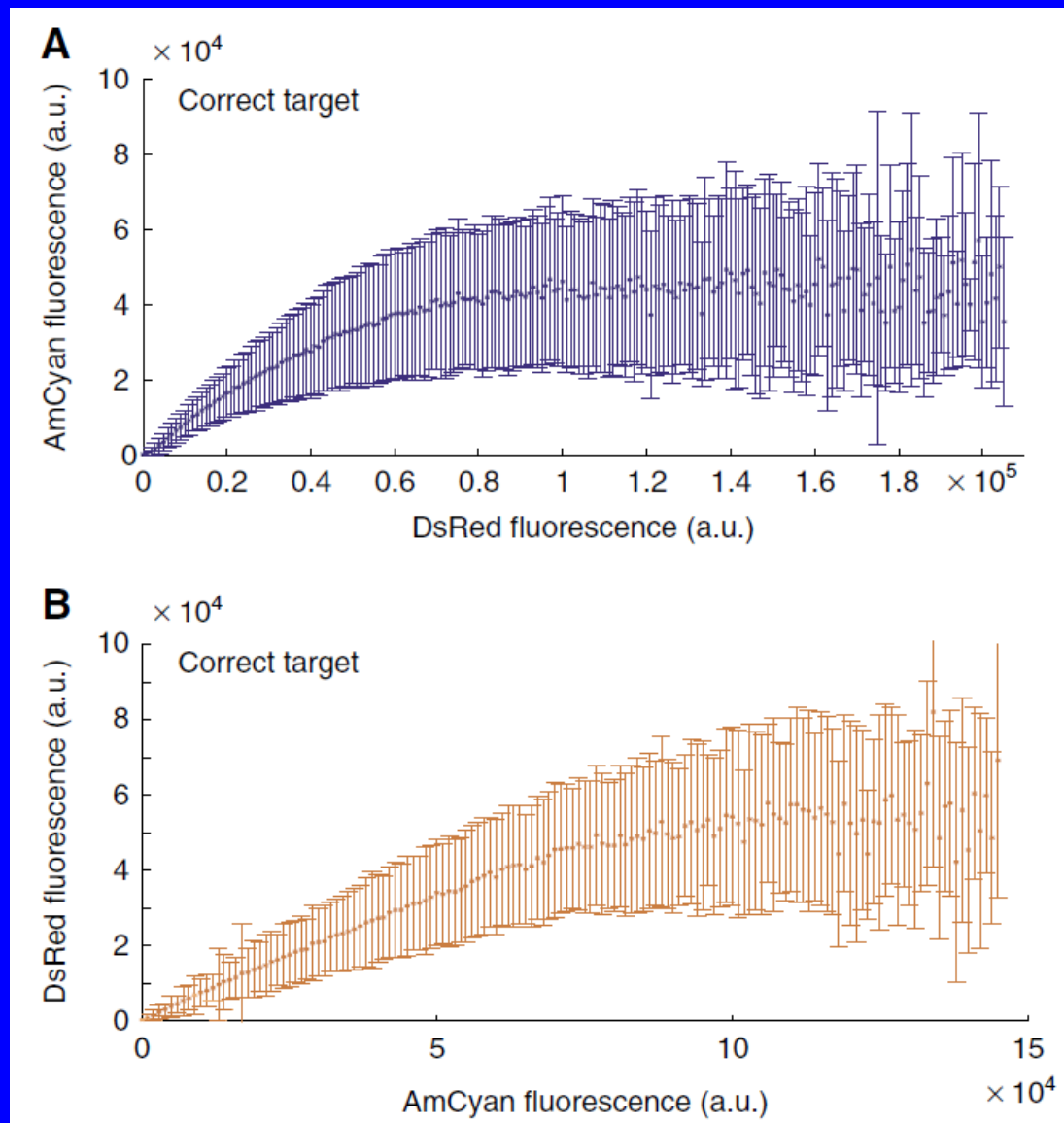
**C**

Circuit:





Experimental results with tI1-FFL motifs



Experimental results obtained with ptI1-FFLI and ptI1-FFLII motifs

Summary II

We show that synthetic incoherent feedforward motifs can function as adaptive expression units in mammalian cells. Both transcriptional and post-transcriptional implementations exhibit adaptation to the amount of their genetic template, pointing to a universal property of this particular topology.

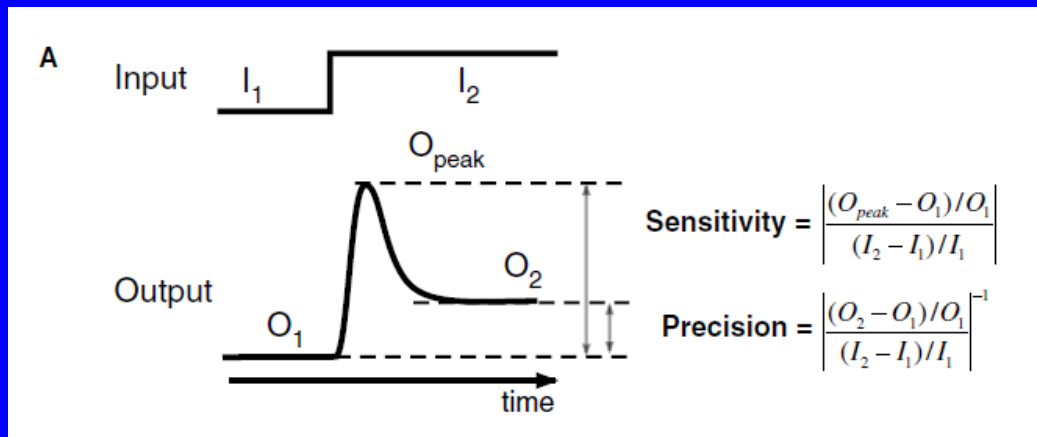
Defining Network Topologies that Can Achieve Biochemical Adaptation

Despite the apparent complexity of cellular networks, there might only be a limited number of network topologies that are capable of robustly executing any particular biological function.

We ask if there are finite solutions for achieving adaptation. What are all network topologies that are capable of robust adaptation?

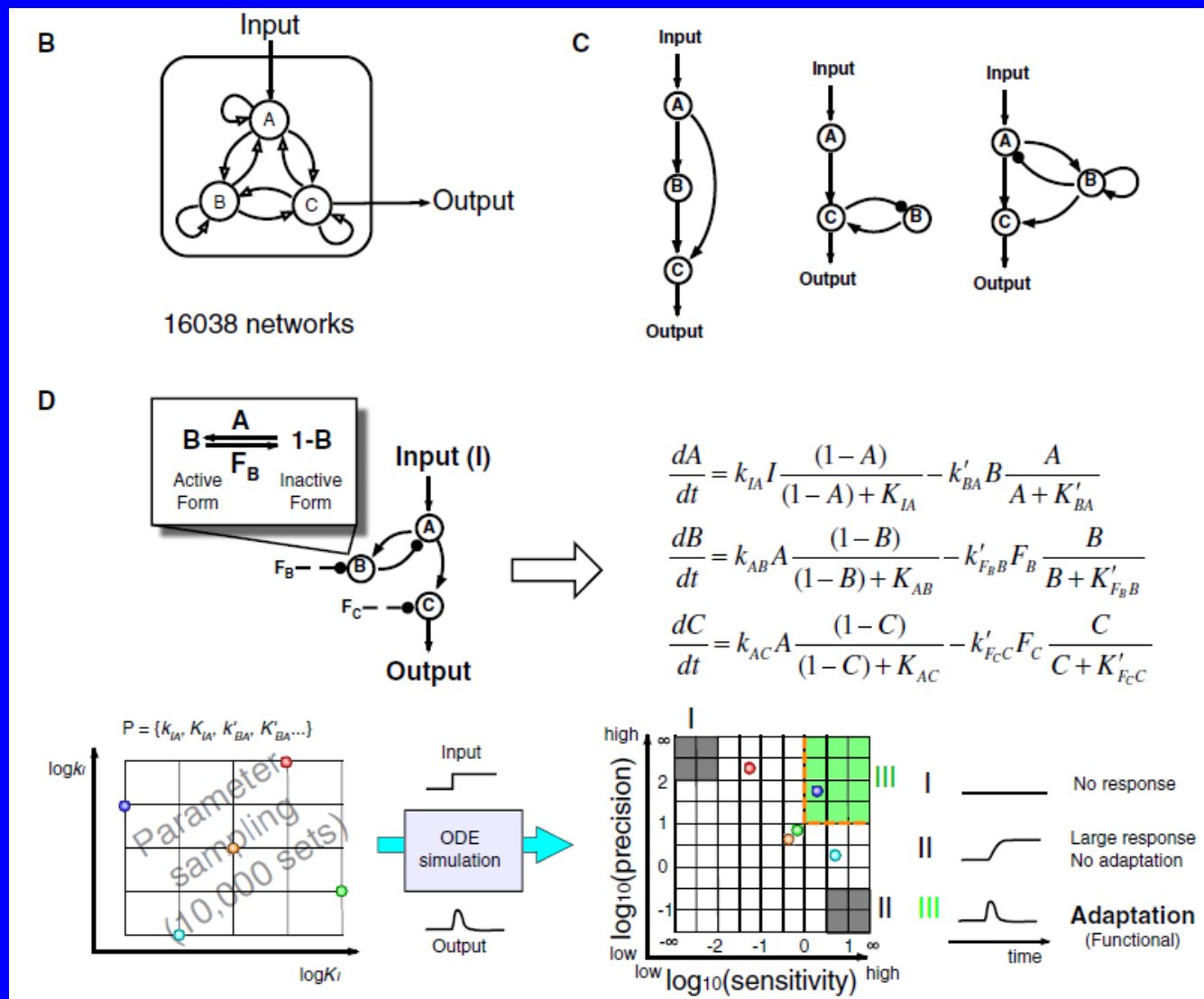
Ma W, Trusina A, El-Samad H, Lim WA, Tang C. .2009; 138(4): 760-73.

Defining quantities to characterize perfect adaptation: sensitivity and precision



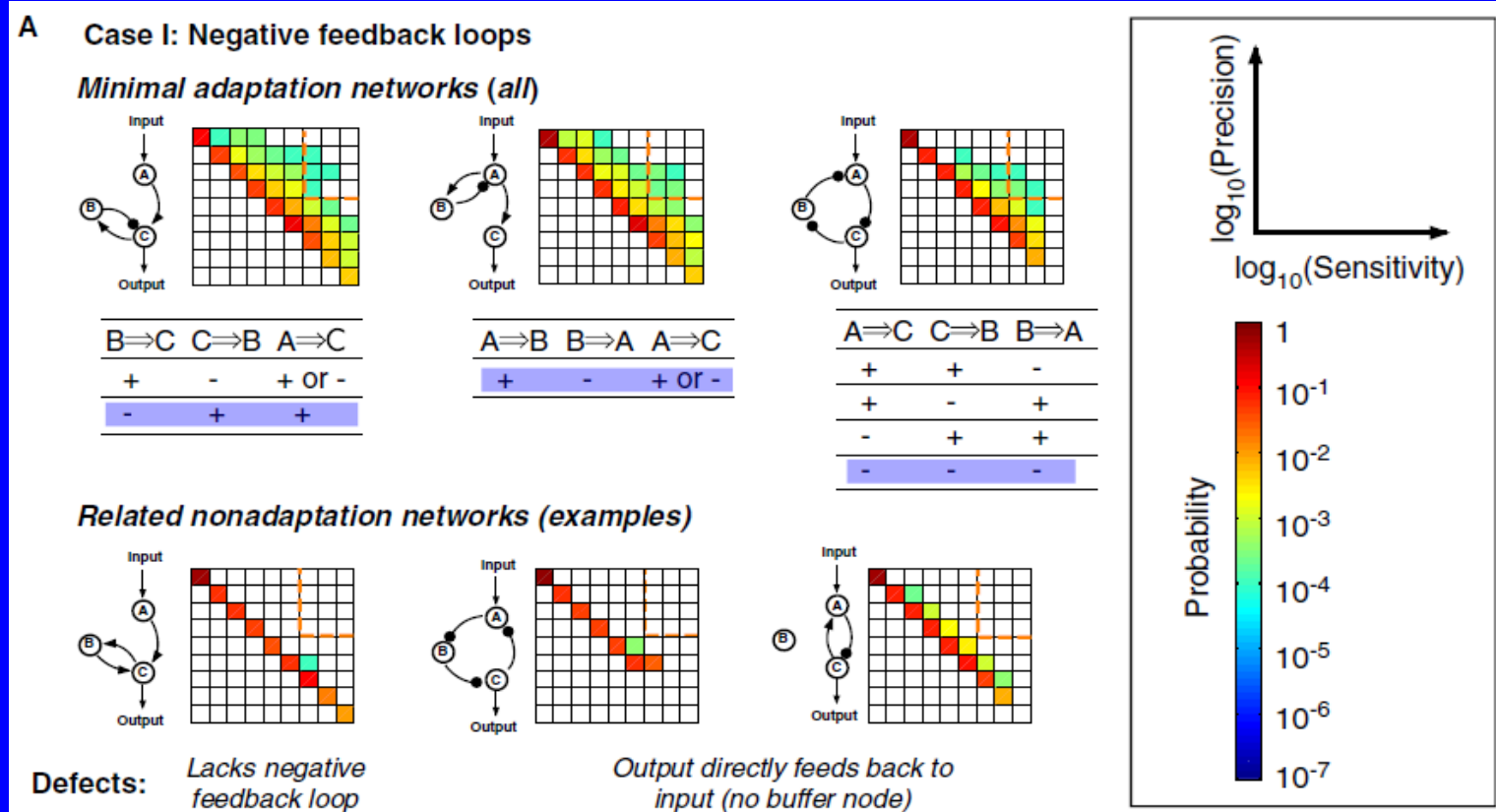
***Perfect adaptation:
sensitivity > 1
precision > 10.***

Sensitivity is defined as the height of output response relative to the initial steady-state value. Adaptation precision represents the difference between the pre- and poststimulus steady states, defined here as the inverse of the relative error.



- (B) Possible directed links among three nodes.
- (C) Illustrative examples of three-node circuit topologies.
- (D) Illustration of the analysis procedure for a given topology.

Minimal Networks Capable of Adaptation

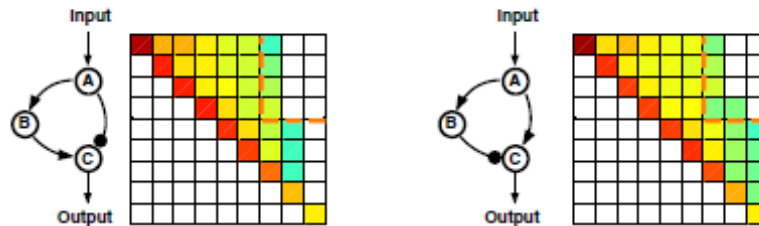


(A) Adaptive networks composed of negative feedback loops. Three examples of adaptation networks are shown in the upper panel. For comparison, three examples of nonadaptive networks are shown in the lower panel, with their “defects” for adaptation function listed underneath.

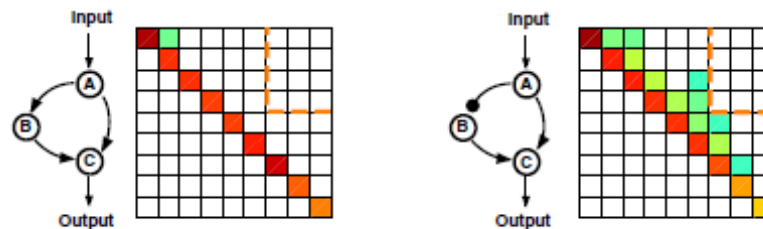
B

Case II: Incoherent feed-forward loops

Minimal adaptation networks (all)



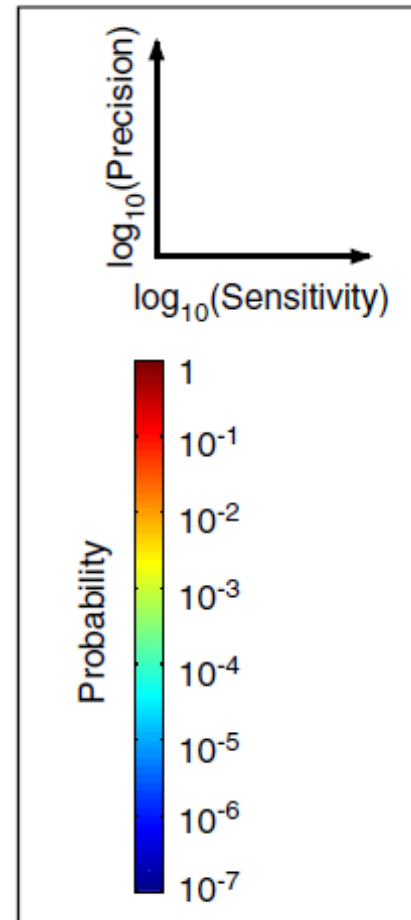
Related nonadaptation networks (example)



Defects:

*Lacks incoherent
feed-forward loop
(only coherent)*

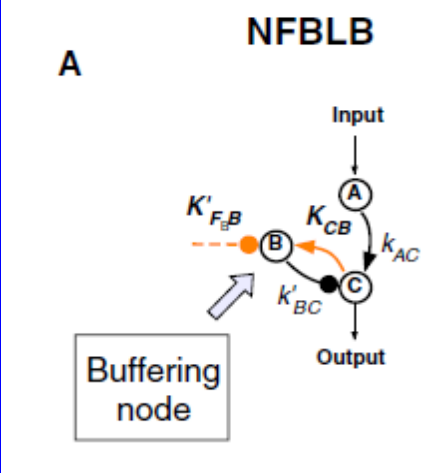
*A to C and B to C
have the same sign*



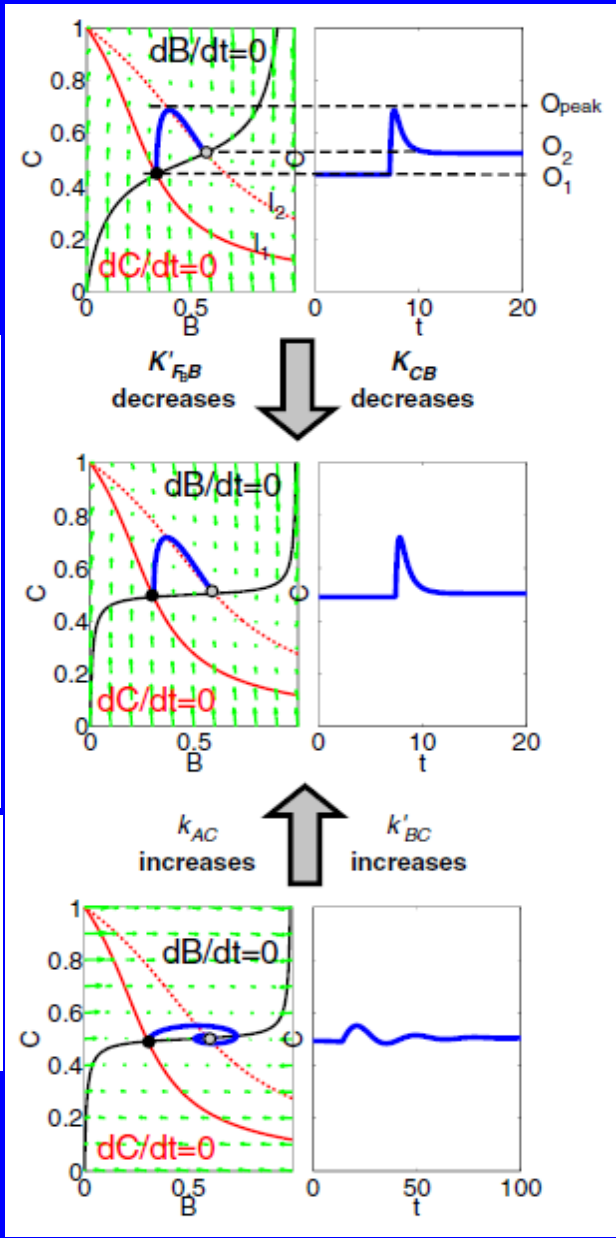
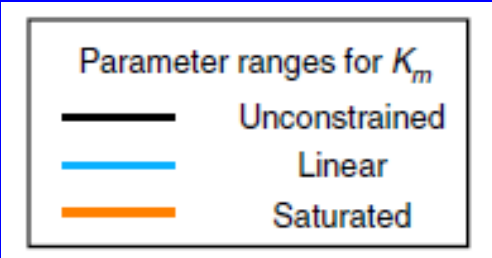
(B) Adaptive networks composed of incoherent feedforward loops. The only two minimal adaptation networks in this case are shown in the upper panel. Examples of nonadaptive networks are shown in the lower panel.

Figure 3: Phase Diagram and Nullcline Analysis of Representative Networks.

$$\begin{aligned}\frac{dA}{dt} &= Ik_{IA} \frac{(1-A)}{(1-A) + K_{IA}} - F_A k'_{FAA} \frac{A}{A + K'_{FAA}} \\ \frac{dB}{dt} &= Ck_{CB} \frac{(1-B)}{(1-B) + K_{CB}} - F_B k'_{FBB} \frac{B}{B + K'_{FBB}} \\ \frac{dC}{dt} &= Ak_{AC} \frac{(1-C)}{(1-C) + K_{AC}} - Bk'_{BC} \frac{C}{C + K'_{BC}}\end{aligned}$$



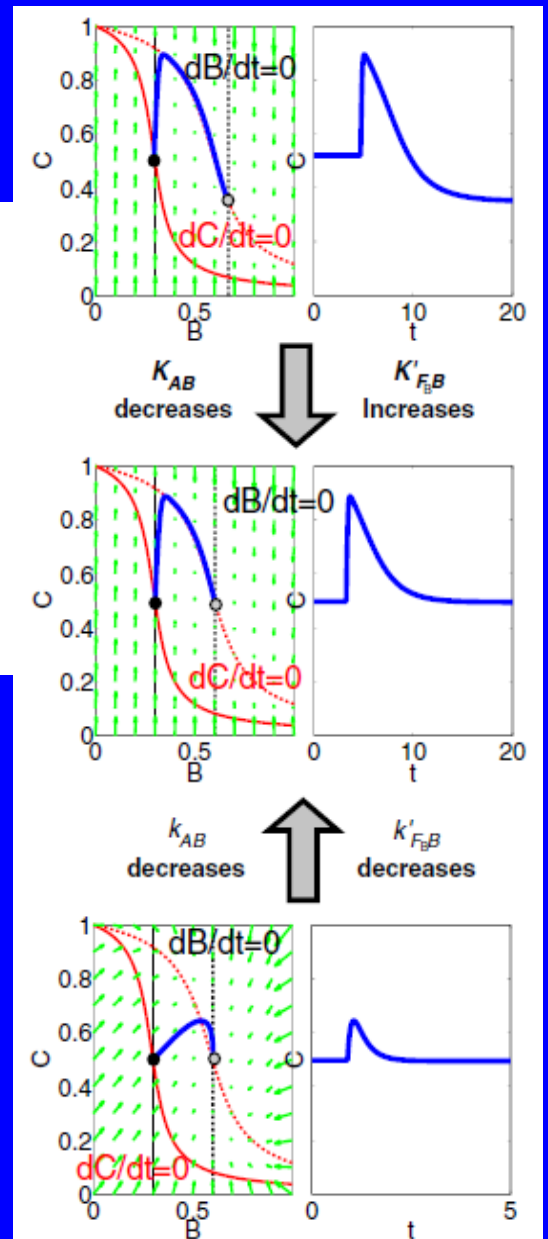
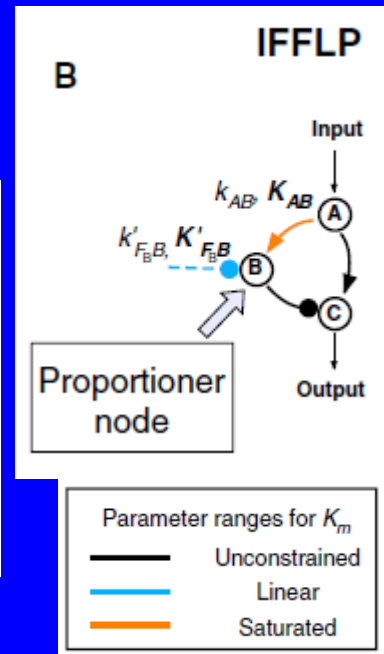
Phase planes of the variables B and C for a NFBLB topology.



$K'_{F_B B} = 0.1$ and $K_{CB} = 0.1$ for the top panel and $K'_{F_B B} = 0.01$ and $K_{CB} = 0.01$ for the middle and lower panels. Two sets of rate constants are used to illustrate their effect on sensitivity: $k_{AC} = 10$ and $k'_{BC} = 10$ for the top and the middle panels and $k_{AC} = 0.1$ and $k'_{BC} = 0.1$ for the lower panel.

Phase planes for an IFFLP topology

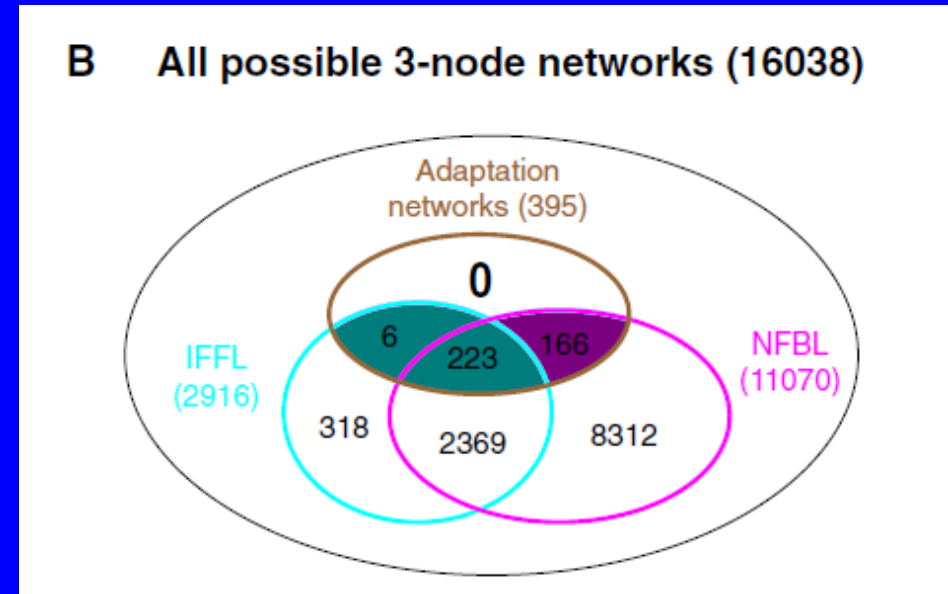
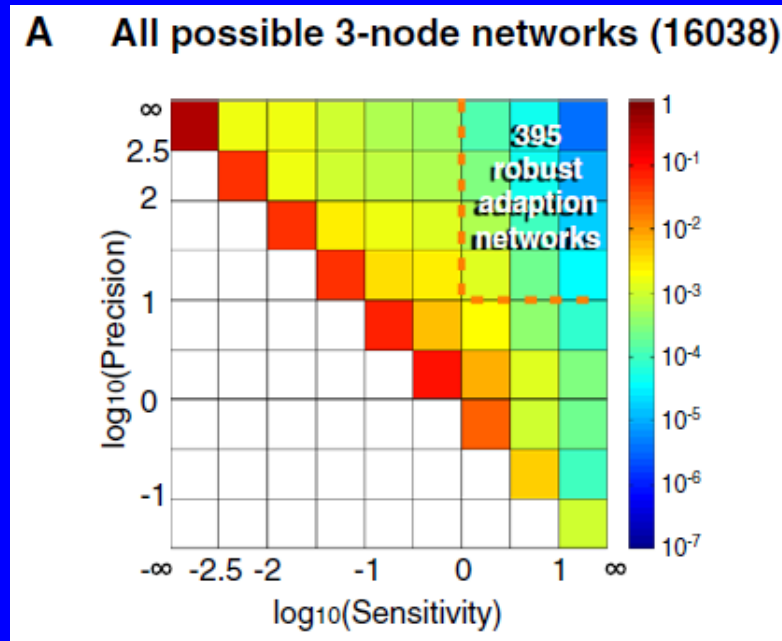
$$\begin{aligned}\frac{dA}{dt} &= I k_{IA} \frac{(1-A)}{(1-A) + K_{IA}} - F_A k'_{FAA} \frac{A}{A + K'_{FAA}} \\ \frac{dB}{dt} &= A k_{AB} \frac{(1-B)}{(1-B) + K_{AB}} - F_B k'_{FBB} \frac{B}{B + K'_{FBB}} \\ \frac{dC}{dt} &= A k_{AC} \frac{(1-C)}{(1-C) + K_{AC}} - B k'_{BC} \frac{C}{C + K'_{BC}}.\end{aligned}$$



Node B to serve as a proportioner for node A—i.e., node B is activated in proportion to the activation of node A and to exert opposing regulation on node C.

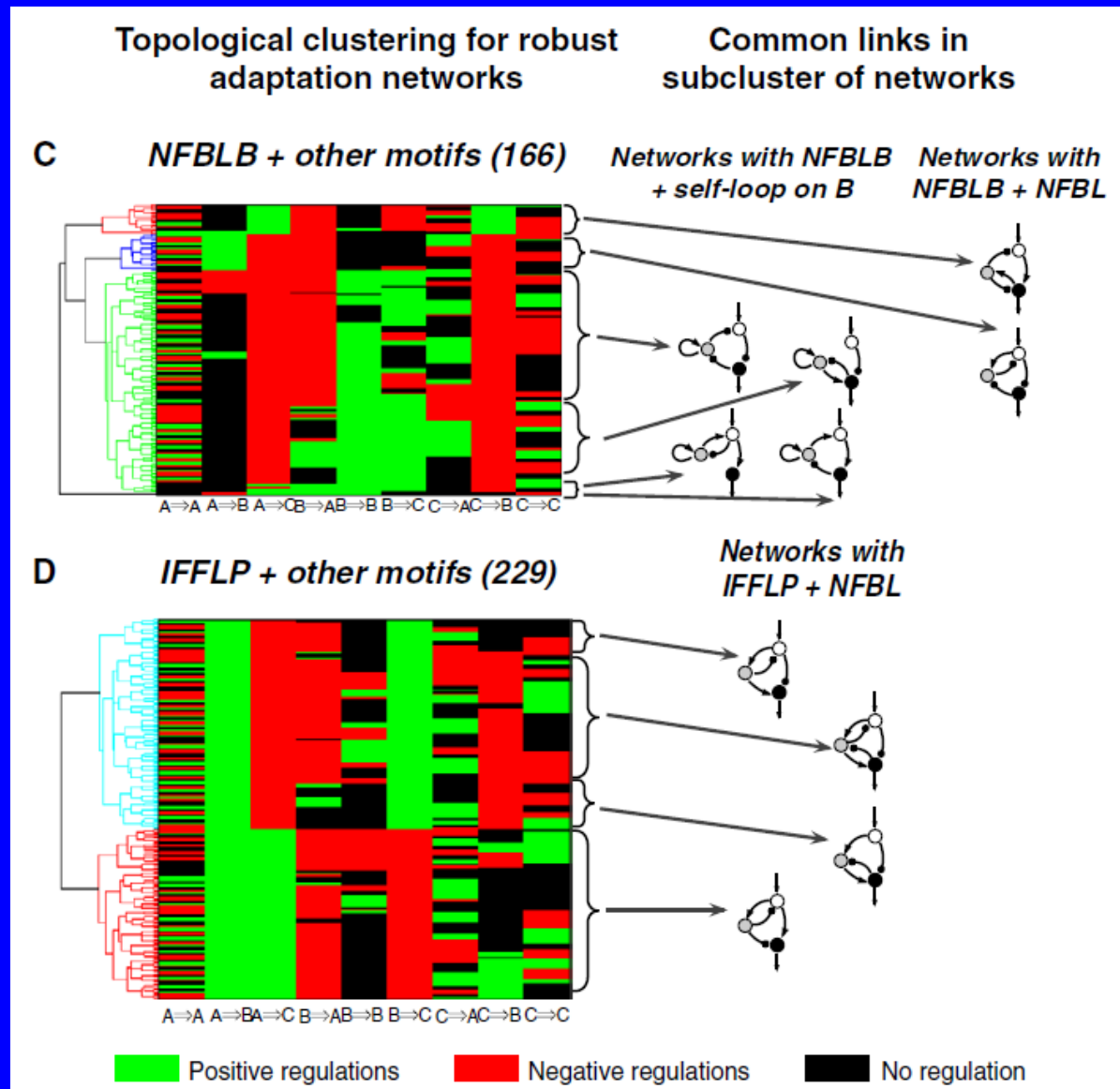
(B) Phase planes for an IFFLP topology. $K'_{FBB} = 1$ and $K_{AB} = 0.1$ for the top panel. $K'_{FBB} = 100$ and $K_{AB} = 0.001$ for the middle and the lower panels. $k_{AB} = 0.5$ and $k'_{FBB} = 10$ for the top and the middle panels. $k_{AB} = 100$ and $k'_{FBB} = 2000$ for the lower panel.

Figure 4. Searching the Full Circuit-Space for All Robust Adaptation Networks



(A) The probability plot for all 16,038 networks with all the parameters sampled.

(B) Venn diagram of networks with three characters: adaptive, containing negative FBL, and containing incoherent FFL.



(C) Clustering of the adaptation networks that belong to the NFBLB class. (D) Clustering of adaptation networks that belong to the IFFLP class.

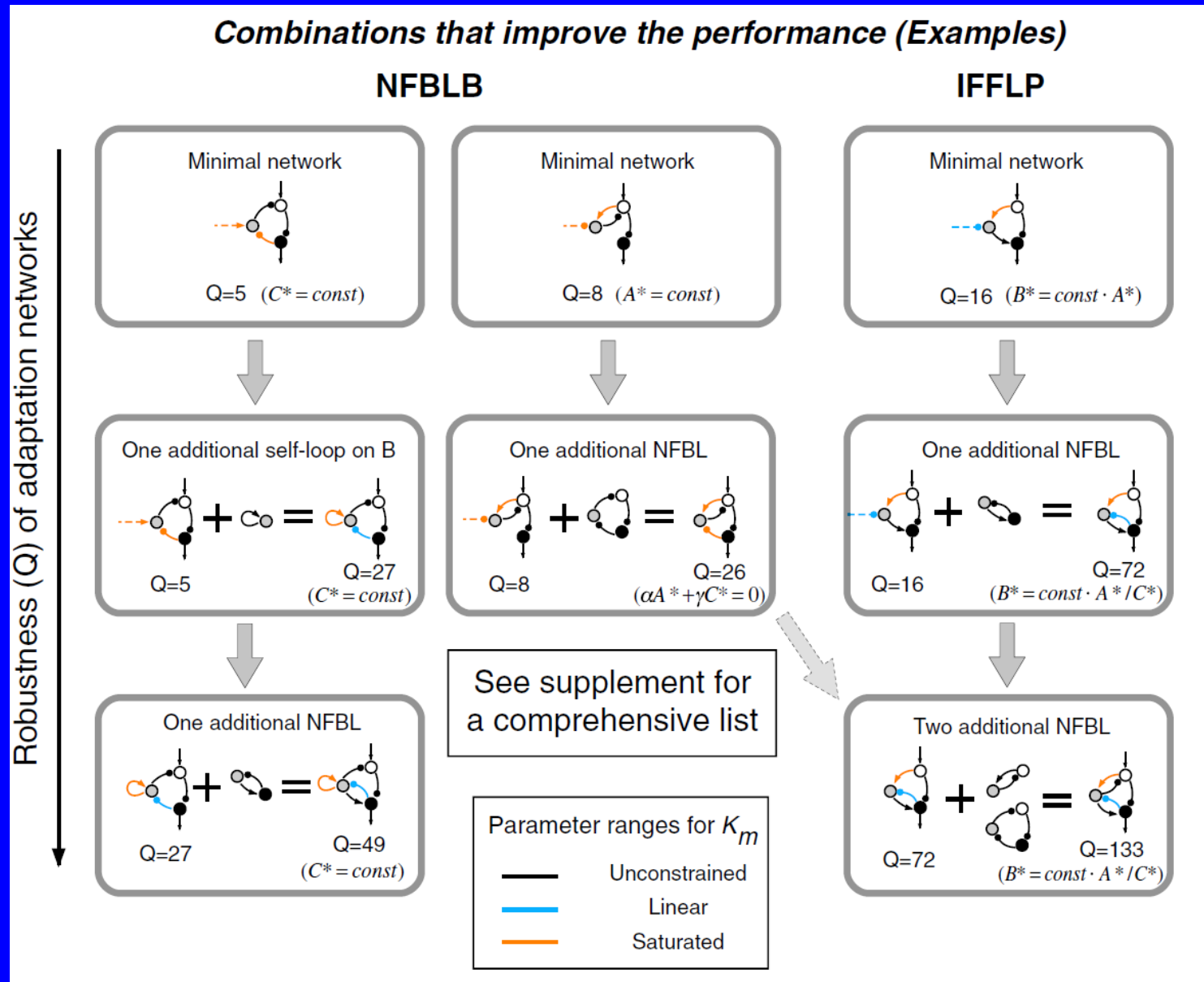


Figure 6. Design Table of Adaptation Networks

Biological Examples of Adaptation

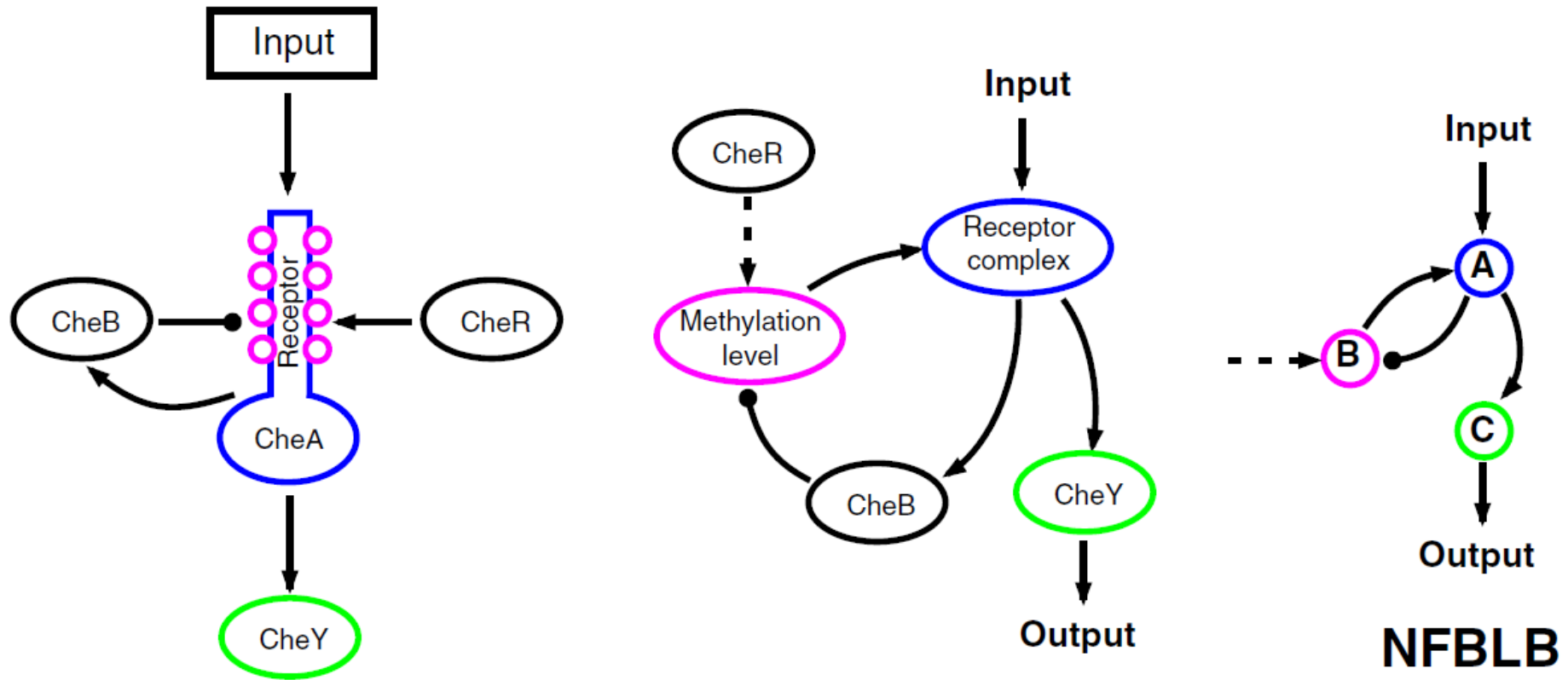


Figure 7. The Network of Perfect Adaptation in E. coli Chemotaxis Belongs to the NFBLB Class of Adaptive Circuits

No IFFLP is found in real biological systems!

Does IFFLP topology have some intrinsic differences concerning adaptation from NFBLB that are not captured by our study?

Is it harder to implement in real biological systems?

Or, do we simply have to search more biological systems?

Summary III

Only two major core topologies emerge as robust solutions: a negative feedback loop with a buffering node and an incoherent feedforward loop with a proportioner node.

Minimal circuits containing these topologies are, within proper regions of parameter space, sufficient to achieve adaptation.

More complex circuits that robustly perform adaptation all contain at least one of these topologies at their core.

Assignment 6

Reproducing Fig.3 in the following literature:

Ma, W., A. Trusina, et al. (2009). "Defining Network Topologies that Can Achieve Biochemical Adaptation." 138(4): 760-773.

Pointing out:
Sensitivity and Precision

